Short Heparin Sequences Spaced by Glycol-Split Uronate Residues Are Antagonists of Fibroblast Growth Factor 2 and Angiogenesis Inhibitors†

Benito Casu,*,‡ Marco Guerrini,‡ Annamaria Naggi,‡ Marta Perez,‡ Giangiacomo Torri,‡ Domenico Ribatti,§ Paolo Carminati,|| Giuseppe Giannini,|| Sergio Penco,|| Claudio Pisano,|| Mirella Belleri,⊥ Marco Rusnati,⊥ and Marco Presta⊥

G. Ronzoni Institute for Chemical and Biochemical Research, 20133 Milan, Italy, Department of Anatomy, University of Bari, Sigma-Tau Research Department, Pomezia, Rome, Italy, and Unit of General Pathology and Immunology, Department of Biomedical Sciences and Biotechnology, School of Medicine, University of Brescia, 25123 Brescia, Italy

Received February 11, 2002; Revised Manuscript Received May 17, 2002

ABSTRACT: Fibroblast Growth Factor-2 (FGF2) is a major inducer of neovascularization (angiogenesis). Heparin activates FGF2 by favoring formation of ternary complexes with its cellular receptors (FGFRs). Controlled 2-*O*-desulfation followed by exhaustive periodate oxidation/borohydride reduction has been used to generate sulfation gaps within the prevalent heparin sequences, building-up arrays of pentasulfated trisaccharides (PST, consisting of a 2-*O*-sulfated iduronic acid flanked by two *N*,6-disulfated glucosamines) spaced by reduced, glycol-split uronic acid (sU) residues. The structure of the prevalent sequences of the novel heparin derivative has been confirmed by mono- and two-dimensional NMR analysis. NMR spin−lattice relaxation times (T_2) and nuclear Overhauser effects suggest that the sU residues act as flexible joints between the PST sequences and cause a marked distortion of the chain conformation of heparin required for formation of ternary complexes. Since the splitting reaction also occurs at the level of the essential glucuronic acid residue of the active site for antithrombin, the heparin derivative has no anticoagulant activity. However, it fully retains the FGF2-binding ability of the original heparin, as shown by its capacity to protect FGF2 from trypsin cleavage and to prevent the formation of heparan sulfate proteoglycan (HSPG)/FGF2/FGFR1 ternary complexes. However, when compared to heparin it showed a reduced capacity to induce FGF2 dimerization and to favor the interaction of [^{125}I]FGF2 with FGFR1 in HSPG-deficient, FGFR1-transfected CHO cells. Accordingly, it was more effective than heparin in inhibiting the mitogenic activity exerted by FGF2 in cultured endothelial cells. Finally, it inhibited angiogenesis in a chick embrio chorioallantoic membrane (CAM) assay in which heparin is inactive.

Basic Fibroblast Growth Factor (FGF2)[1] is a potent angiogenic molecule belonging to a family of heparin-binding proteins (*1*, *2*). FGFs use a dual receptor system to exert their cellular effects. The signal transducing component is a family of tyrosine-kinase FGF receptors (FGFRs). The other component is the glycosaminoglycan (GAG) moiety of a heparan sulfate proteoglycan (HSPG). FGF2 is inactive in normal tissue and becomes activated upon tissue injury, inflammation or tumor invasion. The enzyme heparanase releases the growth factor from HS chains and also generates heparin-like HS fragments that bind to (and activate) FGF2 (*3*, *4*). Activation of FGF2 occurs through its dimerization (*5*, *6*), which in turn facilitates FGFR dimerization and transmembrane signaling (*7*−*9*). FGF2 can be also activated by exogenous heparin (*3*, *8*). Conceivably, favoring of FGF2 and FGFR oligomerization and mitogenic signaling are at the basis of the pro-angiogenic activity of heparin in a chick embrio chorioallantoic membrane (CAM) model in the absence of angiostatic substances such as corticosteroids (*10*).

The structure of heparin is largely comprised of regular trisulfated disaccharide (TSD) sequences made up of alter-

† This work was supported in part by grants from the Associazione Italiana per la Ricerca sul Cancro, Istituto Superiore di Sanità (AIDS Project), National Research Council (Target Project on Biotechnology), Ministero dell'Università e della Ricerca Scientifica e Tecnologica (Centro di Eccellenza IDET, and Cofin 2000) to M.P. and Cofin 2000 to M.R.

* To whom correspondence should be addressed.
‡ G. Ronzoni Institute for Chemical and Biochemical Research.
§ Department of Anatomy.
|| Sigma-Tau Research Department.
⊥ Unit of General Pathology and Immunology.

[1] Abbreviations: FGF2, basic fibroblast growth factor; GAG, glycosaminoglycan; FGFR, tyrosine kinase receptor; HS, heparan sulfate; HSPG, heparan sulfate proteoglycan; IdoA, L-iduronic acid; IdoA2SO_3, L-iduronic acid 2-sulfate; GlcA, D-glucuronic acid; GalA, L-galacturonic acid; aGulA, 2,3-anhydro guluronic acid; sU, split uronic acid; GlcN, D-glucosamine; GlcNSO_3, D-glucosamine *N*-sulfate; Glc$NSO_3$6SO_3, D-glucosamine *N*.6-sulfate; GlcNSO_3, D-glucosamine *N*-sulfate; GlcN,3,-6SO3, D-glucosamine *N*.3.6-sulfate; GlcNAc, *N*-acetyl-D-glucosamine; GlcNAc6SO_3, *N*-acetyl-D-glucosamine 6-sulfate; PST, pentasulfated trisaccharide; p-PST·U, poly-pentasulfated trisaccharide·uronic acid; p-PST·sU, poly-pentasulfated trisaccharide·split uronic acid; GPC-HPLC, gel permeation chromatography-high performance liquid chromatography; NMR, nuclear magnetic resonance; 1D, one-dimensional; 2D, two-dimensional; COSY, correlation spectroscopy; TOCSY, total correlation spectroscopy; DQF, double quantum filter; TPPI, time-proportional phase incrementation; HSQC, heteronuclear single-quantum coherence; HMBC, heteronuclear multiple-bond correlation; INEPT, insensitive nuclei enhanced by polarization; CPMG, Carr-Purcell-Meiboom-Gill sequence; NOE, nuclear Overhauser effect: NOESY, nuclear Overhauser effect spectroscopy; CAM, chicken chorioallantoic membrane.

10.1021/bi020118n CCC: $22.00
Published on Web 07/23/2002

nating, α-1,4-linked residues of 2-*O*-sulfated L-iduronic acid ($IdoA2SO_3$) and *N*,6-disulfated D-glucosamine ($GlcNSO_3$,-$6SO_3$). These sequences are generated by the action of several enzymes on the biosynthetic precursor *N*-acetyl heparosan which consists of nonsulfated D-glucuronic acid (GlcA) residues *β*-1,4-linked to *N*-acetylated α-D-glucosamine (GlcNAc). The TSD sequences of heparin are occasionally interrupted by nonsulfated uronic acids (either GlcA or IdoA) and by undersulfated hexosamines ($GlcNSO_3$, GlcNAc, $GlcNAc6SO_3$). 3-*O*-Sulfated glucosamines ($GlcNSO_33SO_3$ or $GlcNSO_33,6SO_3$) are minor but important constituents of heparin, since they are part of the pentasaccharidic binding site for antithrombin (AT), essential for the expression of significant anticoagulant activity (*11*, *12*). HS, which is also biosynthesized starting from *N*-acetyl heparosan, is more heterogeneous and less sulfated than heparin. It chiefly contains GlcA and GlcNAc residues together with minor, heparin-like sequences (*12*).

The structure and minimal size of heparin (and HS) chains able to bind to FGFs (especially to FGF2) has been extensively investigated using both natural fragments (*13*−*15*) and synthetic oligosaccharides (*16*, *17*). Whereas oligosaccharides as small as tetrasaccharide bind to FGF2 (*5*, *18*, *19*), chains longer than octa-decasaccharides are necessary for mitogenic activity (*5*, *8*, *9*, *20*). Also some undersulfated heparin oligosaccharides (missing, i.e., 6-*O*-sulfate groups on aminosugar residues) are able to bind to FGF2 (*13*−*15*).

The X-ray structures of tetra- and hexasaccharide−FGF2 complexes indicate that the minimum FGF2-binding heparin structure consists of a NSO_3 group (NS) and a 2-OSO_3 group (2S) on contiguous GlcN and IdoA residues, respectively (*19*). Molecular models clearly show NS/2S pairs on both sides of a heparin helix, irrespective of the conformation of the $IdoA2SO_3$ residues (*21*). These pairs of sulfate groups are also evident when the primary structure of the "regular" sequences of heparin is depicted as repeating tetrasaccharide units **1** (Figure 1), a representation that takes into account the trans orientation of alternate disaccharide units and shows at first glance which substituent groups are close to each other on adjacent residues. As shown by molecular modeling (*8*, *20*, *22*) and X-ray diffraction studies (*7*, *8*, *23*), relatively long arrays of NS/2S pairs are necessary for binding more than one FGF2 molecule and formation of signal-transducing heparin/FGF/FGFR complexes. It was of interest to investigate whether the structure of heparin could be modified such that, while retaining the ability of the polysaccharide to bind 1:1 to FGF2, dimerization of FGF2 and formation of FGF2/FGFR complexes could be largely inhibited. With the aim of obtaining FGF2 inhibitors, we have generated sulfation gaps along the regular heparin sequences by selectively removing 2S groups to reach a ratio of about 1:1 between sulfated and nonsulfated uronic acid residues. To disrupt the original helical chain conformation, the C(2)−C(3) bonds of all nonsulfated uronic acid residues have been split, generating flexible joints along the heparin chains while minimizing cleavage of glycosidic bonds. The novel heparin derivative retains the FGF2-binding ability of the parent heparin. Although it is a poor inducer of FGF2 dimerization, it is a better inhibitor than heparin of the FGF2-induced growth of endothelial cells and is antiangiogenic in an established chick embryo chorioallantoic membrane (CAM) assay.

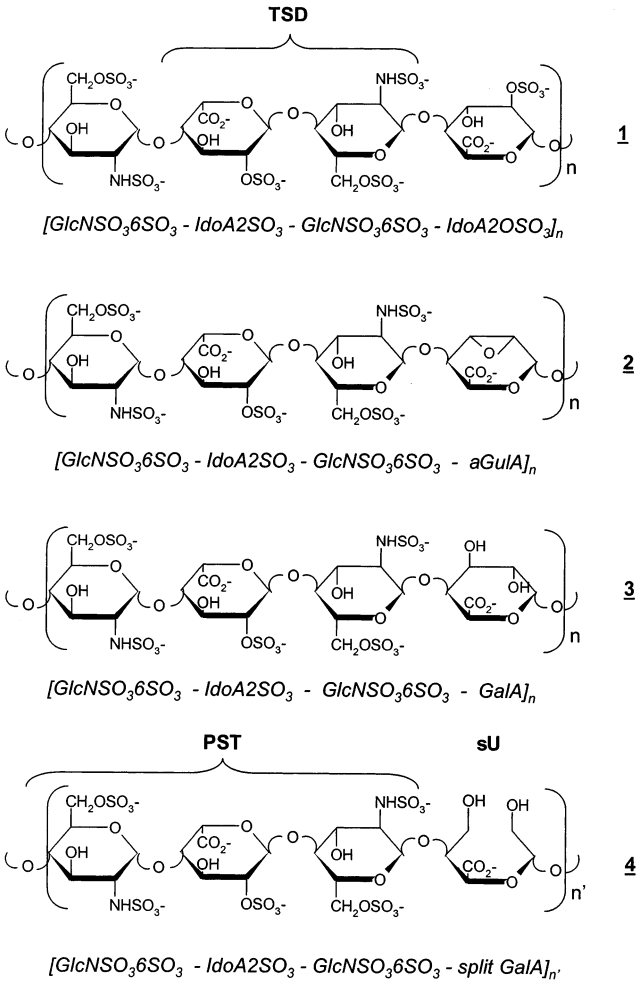

FIGURE 1: Prevalent sequences in regular regions of heparin and chemically modified heparins. **1**, heparin; **2**, partially epoxidated heparin; **3**, 50% 2-*O*-nonsulfated heparin (prevalently p-PST·U sequences); **4**, 50% 2-*O*-desulfated and glycol-split heparin (prevalently p-PST·sU sequences).

EXPERIMENTAL PROCEDURES

Materials. Porcine mucosal heparin sodium salt (170 IU/mg, FU IX) was prepared by Laboratorio Derivati Organici (Trino Vercellese, Italy). Sulfation pattern, by ^{13}C NMR (*24*): $IdoA2SO_3$ 65.6%; GlcA + IdoA 34.4%; GlcN *N*-sulfation 86.0%; GlcN 6-*O*-sulfation 78.4%. Average molecular weights, by GPC−HPLC (*25*): Mn 15 500; Mw 17 000; polydispersion = 1.1. Beef lung heparin used as a reference for NMR relaxation mesuraments (Mw 12 000) was prepared by Hepar. *N*-Acetyl heparin was prepared as previously described (*26*). Human recombinant FGF2 was purified from *Escherichia coli* cell extract by heparin-Sepharose affinity chromatography as described by Isacchi et al. (*27*).

Preparation of Reduced Oxyheparin (RO−Heparin). RO−heparin was prepared essentialy as described in ref *28*. Briefly, 1 g of heparin dissolved in 25 mL of distilled water was added at 4 °C of 25 mL of $NaIO_4$ 0.2 M; the solution was stirred in the dark for 20 h, addded of ethylene glycol, desalted by tangential ultrafiltration, added of 400 mg of $NaBH_4$, stirred for 3 h at room temperature, neutralized with diluted HCl and desalted by tangential ultrafiltration.

Preparation of Partially 2-O-Desulfated Heparin. Heparin selectively *O*-desulfated at C2 of the IdoA residue was

prepared by alkaline treatment of heparin following a modification of the methods of Perlin et al. (*29*, *30*). Heparin (4 g) was dissolved in 25 mL of water at 60 °C. A total of 25 mL of 2 M NaOH were added to the solution. After stirring for 30−45 min at 60 °C, the reaction was stopped by cooling, and the solution brought to pH 7 with HCl. The product (heparin epoxide, with 21% epoxidation as determined by ^{13}C NMR) (*31*) was isolated by freeze-drying, dissolved in 75 mL of water and heated for 48 h at 70 °C. (Yield: about 85%.)

Exhaustive Glycol-Splitting of Partially 2-O-Desulfated Heparin. Partially 2-*O*-desulfated heparin was periodate-oxidized and reduced essentially as described for heparin (*28*). The final product, chiefly p-PST·sU, Mw 9800 (see text), was recovered by freeze-drying. (Yield: about 65% as referred to the starting 2-*O*-desulfated heparin.)

NMR Spectroscopy. The 1D and 2D spectra were obtained at 500 MHz for ^{1}H and 125 MHz for ^{13}C, with a Bruker AMX spectrometer, equipped with a 5-mm 1H/X inverse probe, from D_2O solutions (15 mg/0.5 mL D_2O, 99.99% D), or, for long experiments, from buffer solutions (10 mM phosphate buffer, pH 7, in D_2O). Chemical shifts, given in parts per million downfield from sodium-3-(trimethylsilyl)-propionate, were measured indirectly with reference to acetone in D_2O (δ 2.235 for ^{1}H and δ 30.20 for ^{13}C). Experiments were performed at 45 °C on samples treated with EDTA (*32*) to avoid signal shifts and broadening caused by the presence of trace divalent cations. (EDTA was removed by gel filtration on Sephadex G25 before the spectral measurements.) The ^{1}H, COSY, and TOCSY spectra were obtained with presaturation of the HOD signal. ^{13}C spectra for monitoring reaction kinetics were obtained at 100 MHz with a Bruker AMX400 spectrometer equipped with a multinuclear 10-mm probe, from D_2O solutions (100 mg/mL).

The DQF−COSY and 2D-TOCSY spectra were obtained with presaturation of the HOD signal and 16 scans/each free induction decays were used. The ^{1}H/^{13}C chemical shift correlation (HSQC) (*33*) and HMBC (*34*) spectra were performed using *z*-gradients for coherence selection. The HSQC spectrum was obtained with carbon decoupling during acquisition period in phase sensitivity-enhanched pureabsorption mode. The matrix size was 1K × 512 points and the experiment was zero-filled to 2K × 1K and multiplied with shifted (π/3) sine-bell-squared prior Fourier transformation. The HMBC spectrum was acquired using 128 scans series in 1K × 256W data points. The spectrum was optimized for a $^{n}J_{C-H}$ of 6 Hz, with $n = 2-4$.

The spin−spin relaxation times T_2 were determined using a modified double INEPT sequence, with suppression of the effects of cross-relaxation between dipolar and chemical shift anisotropy relaxation mechanism (*35*). The CPMG pulse trains were 4.5−9.0−18.2−36.2−54.3−72.4, and 90.5 ms. A shifted sine-bell-squared function was applied before Fourier transformation of each T_2 experiment. The cross-peak volumes were measured using the Bruker UXNMR software package running on a Silicon Graphics Indy workstation. The 2D-NOESY spectra were measured at 500 MHz at 40 °C, with mixing times of 50, 100, 150, 200, and 250 ms and presaturation of the residual HOD signal. The 2D experiments matrix size of 1K × 256 was zero filled to 4K × 2K by application of a squared cosine function before Fourier transformation.

Computational Methods. Modeling calculations were performed with MacroModel V7.0 software package running on a Silicon Graphics SGO2 workstation, and the AMBER* force field was used for energy calculations (*36*). Conformational searching was made using the Pollack-Ribiere minimization procedure with 1000 trial structures, starting with the geometry of the glycosidic linkages reported for heparin (*21*).

Proteolytic Digestion of FGF2. The protective effect of heparin derivatives on tryptic digestion of FGF2 was evaluated as described by Coltrini et al. (*37*). Briefly, 1-μg aliquots of FGF2 were incubated at 37 °C with trypsin in the presence of the GAG and its integrity was quantified by SDS−PAGE followed by computerized image analysis of the gel.

[^{125}I]FGF2 Dimerization. Human recombinant FGF2 was labeled with Na^{125}I (37 GBq/mL; Amersham International, Amersham, U.K.) using Iodogen (Pierce Chemical, Rockford, IL) as described (*27*). Two nanograms of [^{125}I]FGF2 was incubated for 2 h at 37 °C in PBS in the absence or in the presence of increasing concentrations of heparin derivatives. Then, [^{125}I]FGF2 dimers were cross-linked by adding 1 mM bis[2-(succinimido-oxycarbonyloxy)-ethyl]sulfone (BSOCOES, Pierce Chem. Co.). After 30 min, samples were added with reducing sample buffer, boiled, and loaded onto a SDS−10% polyacrylamide gel. Gels were dried and exposed to Kodak X-OMAT AR film (Eastman Kodak Co., Rochester, NY) at −70 °C. The 36 kDa band, corresponding to [^{125}I]-FGF2 dimer, was quantified by computerized image analysis of the autoradiography using a Magiscan Image Analyzer (Joyce-Loebl LTD, England) with the Genias 3.0 software package.

Cell Cultures. Transformed fetal bovine aortic endothelial GM 7373 cells, corresponding to the described BFA-1c 1BPT multilayered transformed clone (*38*) were obtained from the National Institute of General Medical Sciences, Human Genetic Mutual Cell Repository (Camden, NJ). Cells were grown in Eagle's minimal essential medium containing 10% fetal calf serum (FCS), vitamins, and essential and nonessential amino acids. CHO−K1 cells and A745 CHO cell mutants (kindly provided by J. D. Esko, University of California, San Diego) were grown in Ham's F 12 medium supplemented with 10% FCS. A745 CHO cells harbor a mutation which inactivates the xylosyltransferase that catalyzes the first sugar transfer step in GAG biosynthesis (*39*). The A745 CHO *flg*-1A clone, bearing about 30 000 FGFR1 molecules/cell, has been generated in our laboratory by transfection with the IIIc variant of murine FGFR-1 cDNA (*40*).

FGF2-Mediated Cell−Cell Adhesion Assay. This assay was performed as described (*40*). Briefly, A745 CHO *flg*-1A cells (52 000 cells/cm^2) were added to glutaraldehyde-fixed CHO−K1 monolayers in serum-free medium *plus* 10 mM EDTA with no addition or with 30 ng/mL FGF2 in the absence or in the presence of increasing concentrations of the heparin under test. After 2 h of incubation at 37 °C, A745 CHO *flg*-1A cells bound to the monolayer were counted under an inverted microscope at 125× magnification. Data are expressed as the mean of the cell counts of three microscopic fields chosen at random. All experiments were performed in duplicate and were repeated twice.

[^{125}I]FGF2 Binding to FGFR1. Subconfluent cultures of A745 CHO flg-1A cells were incubated at 4 °C in serum-free medium containing 3 ng/mL of [^{125}I]FGF2, 0.15% gelatin, 20 mM Hepes buffer (pH 7.5), in the presence of increasing concentrations of p-PST·sU or unmodified heparin. After 2 h, the amount of [^{125}I]FGF2 bound to FGFR1 was evaluated as described (*41*).

Cell Proliferation Assays. Cell proliferation assay on GM 7373 cells was performed as described (*42*). In our experimental conditions, control cultures incubated in 0.4% FCS with no addition or with 10 ng/mL FGF2 undergo 0.1−0.2 and 0.7−0.8 cell population doublings, respectively. Cells grown in 10% FCS undergo 1.0 cell population doublings (*42*).

DNA synthesis was evaluated on BAE cells seeded on 96 well plates at 2500 cells/well. After 24 h, cells were incubated in DMEM plus 0.5% FCS for a further 48 h. Then, cells were treated with 30 ng/mL FGF2 in the absence or in the presence of increasing concentrations of the GAG under test without changing the medium. After 16 h, all cell cultures were incubated for further 6 h with [^{3}H]thymidine (1 μCi/mL) and radioactivity incorporated in TCA-precipitable material was counted. In our experimental conditions, radioactivity incorporated in the absence of added GAG was equal to 155 ± 20 and 507 ± 45 cpm/well for control and FGF2-treated cell cultures, respectively.

Chick Embryo Chorioallantoic Membrane (CAM) Assay. Fertilized White Leghorn chick eggs were incubated under conditions of constant humidity at 37 °C. On the third day of incubation, a square window was opened in the egg shell after removal of 2−3 mL of albumen so as to detach the developing CAM from the shell. The window was sealed with a glass of the same size, and the eggs were returned to the incubator. At day 8, 1 mm^3 sterilized gelatin sponges (Gelfoam, Upjohn Company, Kalamazoo, MI) adsorbed with the heparin under test (50−100 μg/embryo) dissolved in 5 μL of PBS were implanted on the top of growing CAMs under sterile conditions (*43*). Sponges containing vehicle alone were used as negative controls. CAMs were examined daily under a Zeiss stereomicroscope SR equipped with the MC 63 Camera System (Zeiss, Oberkochen, Germany). On day 12, blood vessels entering the sponges within the focal plane of the CAM were recognized macroscopically at 50× magnification and counted by two observers in a double-blind fashion (*44*). On the same day, microvascular density at the gelatin sponge-CAM boundary was assessed histologically by a planimetric method of point counting exactly as described (*43*). Mean values ± SD were determined for each analysis.

RESULTS

Synthesis and Structure of the Heparin-Derived Poly-Pentasulfated Trisaccharide (p-PST·sU). Our aim was to quench the FGF2-activating properties of heparin while preserving its capability to bind the growth factor. Our strategy was to generate 2-*O*-sulfation gaps between short sequences of the polysaccharide containing the minimum disaccharide sequence $GlcNSO_3$−$IdoA2SO_3$ binding to FGF2 (*19*, *45*), and then disrupt the original chain conformation by splitting the C(2)−C(3) bonds of all nonsulfated uronic acid residues with periodate (i.e., the original ones and those generated by 2-*O*-desulfation). Conditions for the glycol splitting reaction (with periodate, followed by reduction with borohydride of the resulting dialdehydes) (*28*, *46*) were chosen such as to minimize concomitant cleavage of inter-residue glycosidic bonds, thus largely preserving the original size of the polysaccharide chains. Since the parent pig mucosal heparin already contained over 31% nonsulfated uronic acids (≈22% GlcA and ≈9% IdoA), removal of about 25% of its 2-*O*-sulfate groups was planned in a way to achieve a total of about 55% nonsulfated uronic acids. The reason of targeting slightly over 50% of total nonsulfated uronic acid residues susceptible to glycol splitting relied on the consideration that a significant proportion of GlcA residues of heparin is part of undersulfated, *N*-acetylated regions ("NA blocks") rather than regularly substituting $IdoA2SO_3$ residues in "regular" regions (*12*). Selective 2-*O*-desulfation of heparin can be accomplished by simple lyophylization of a basic solution of heparin (*29*) However, the lyophylization method commonly leads to totally 2-*O*-desulfated heparins. To perform graded *O*-desulfation, in the present work the alternative route of 2-*O*-desulfation in solution (*30*, *31*) was chosen, and experimental conditions were adapted to obtain intermediate heparin epoxides of any desired degree of conversion. The isolated epoxide derivatives were analyzed by ^{13}C NMR (Figure 2b), and experimental conditions were optimized (1 M NaOH, 35 min at

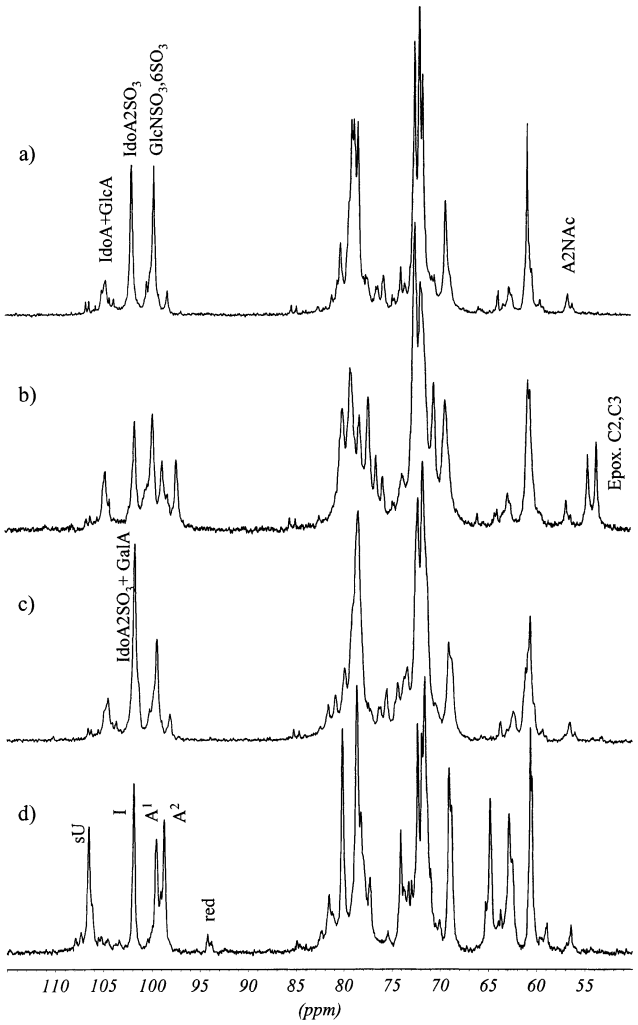

FIGURE 2: ^{13}C NMR spectra (100 MHz, D_2O) of heparin (a) and heparin derivatives **2** (b), **3** (c), and **4** (d).

Table 1: ^{1}H and ^{13}C Chemical Shifts of **4** (prevalent p-PST·sU sequences)

	^{1}H	^{13}C		^{1}H	^{13}C
A^1			I		
1	5.39	99.8	**1**	5.33	102.2
2	3.28	60.7	**2**	4.35	78.7
3	3.77	74.4	**3**	4.21	72.0
4	3.64	77.7	**4**	4.11	79.1
5	4.05	72.1	**5**	4.82	72.2
6	4.2−4.4/3.9	69.1/62.9			
A^2			sU		
1	5.32	98.9	**1**	4.98	106.9
2	3.28	60.7	**2**	3.78−3.68	64.9
3	3.68	72.6	**3**	3.91	62.9
4	3.78	79.1	**4**	4.25	80.4
5	4.01	71.7	**5**	4.64	80.9
6	4.2−4.4/3.9	69.1/62.9			

60 °C) to afford a product with about 32% of the IdoA2SO$_3$ residues in the original sequences **1** converted into 2,3-anhydro-guluronate (aGulA) residues as in sequences **2** (Figure 1). (This degree of conversion corresponds to about 22% of total uronic acids.) The product was then heated 48 h at pH 7 at 60 °C to convert the epoxidated iduronate rings into 2-*O*-desulfated uronic acid (α-L-galacturonic acid, GalA) residues, as confirmed by analysis of ^{1}H and ^{13}C NMR spectra in comparison with the spectra of the corresponding fully modified heparins (*30*, *31*). Integration of relevant ^{13}C signals confirmed that the product prevalently consisted of sequences **3** (GlcNSO$_3$6SO$_3$−IdoA2SO$_3$−GlcNSO$_3$6SO$_3$−GalA)$_n$, i.e., sequences of a pentasulfated trisaccharide (PST) followed by a nonsulfated uronic acid residue (U). Exhaustive periodate oxidation followed by borohydride reduction afforded a final product **4**, Figure 1). The ^{13}C spectrum of **4** is compared in Figure 2 with the spectra of the parent heparin (**1**), the intermediate epoxidic (**2**), and galactosyl-derivative (**3**). The spectrum of **4** is fully compatible with the proposed prevalent structure and with the expected uniform distribution of split residues. It is in fact remarkably clean, showing a major pattern of signals superimposed on minor signals mostly associated with GlcNAc-containing sequences. Also evident in the spectrum are weak signals due to minor reducing end-groups, expected from the somewhat reduced Mw of the product (9800) vs 17 000 for the parent heparin. Independent proof of structure **4** was provided through mild hydrolysis of p-PST·sU, which generated the trisaccharide PST·R (where R is the remnant of a glycol split uronic acid) as a major fragment (unpublished data).

The ^{1}H and ^{13}C chemical shifts of prominent signals of the final product are reported in Table 1 together with the corresponding assignments obtained by analysis of 2D COSY and TOCSY spectra (not shown). Signal patterns were clearly associated to each of the four residues chiefly constituting the novel polysaccharide. The area ratios for the four anomeric signals (^{1}H for two *N*,6-disulfated GlcN residues at 5.39 and 5.32 ppm, and at 5.33 and 4.98 for the two other residues, with corresponding ^{13}C signals at 99.8, 98.9, 102.2, and 106.9) are very close to 1:1:1:1. The ^{1}H anomeric signal of the second residue corresponds to that of IdoA2SO$_3$. The H-2 signal of the fourth residue correlates with protons at 3.78 and 3.68 ppm, respectively, associated with a primary alcohol function, with the corresponding ^{13}C signal at 64.9 ppm. Another set of signals of this latter residue (^{1}H at 3.91 and ^{13}C at 62.4 ppm) correlates with two protons in the TOCSY spectrum, at 4.25 and 4.64 ppm, respectively, its overall signal pattern being the one expected (*47*) for a glycol-split residue sU, with C(1) and C(4) bearing CH_2OH substituents.

The presence of four prevalent residues is clearly shown in the HSQC spectrum of the pPST·sU product (Figure 3a). To confirm that the two glucosamine and the two uronic acids are arranged as in **4**, the position of the interglycosidic linkages was determined by HMBC experiments. The correlations shown in the HMBC spectrum (Figure 3b) indicate connections between H1 of A^1 and A^2 with C4 of I and sU, and between H4 of A^1 and A^2 with C1 of sU and I, respectively. The same correlations across the glycosydic linkages (H1 and H4 of contiguous residues) are also indicated by the 2D NOESY experiments (data in Table 2), thus confirming the predicted sequence. It should be noted that the NMR spectra of the partially 2-*O*-desulfated and exhaustively glycol-split heparin of the present study are deceptively simple and do not fully reflect the structural heterogeneity associated with the presence of different types of glycol-split uronic acid residues. In fact, whereas splitting of the C(2)−C(3) bonds eliminates the stereochemical differences between the *ido* and *galacto* configuration of the precursors (i.e., between the IdoA residues preexisting in unmodified heparin and the GalA residues generated by opening of the epoxide rings), the *gluco* configuration of the original GlcA residues is not modified throughout the epoxidation-epoxide hydrolysis-periodate oxidation−reduction reactions, and NMR signals of glycol-split GlcA and IdoA/GalA are superimposed in the present spectra.

Both experimental NOE effects and carbon spin−spin relaxation times values (T_2) obtained for sequence **4** are compared in Tables 2 and 3 with those for heparin (sequence **1**). T_2 values for most of the overlapping signals, not measurable by classical 1D experiments, were obtained using a modified double INEPT 2D sequence (*35*). The average T_2 values for **4** are twice larger than those calculated for **1**. Although the comparison is not strictly homologous since the Mw of the heparin derivative is somewhat lower than that of the heparin used for relaxation measurements (9800 vs 12 000 Da), the relaxation data strongly suggest that chains made up of sequences **4** are much more flexible than those of the parent polysaccharide. Preliminary molecular modeling calculations indicated that the H1−H5 distance in the sU residue in the favored conformers of **4** is short enough to generate an NOE effect, as actually observed for p-PST·sU (Table 2). By contrast, the most stable conformation of heparin (background model in Figure 4) has measurable NOE effects only for H1 and H4 protons of adjacent residues. The conformer shown in Figure 4, obtained by modeling calculations, is one of the major contributors to the conformation of sequences **4** compatible with the additional NOE effect of 3% observed between protons H1 and H5. Such a conformation clearly involves a drastic distortion of the chain conformation from that of heparin alone (*21*) as well as of heparin oligosaccharides cocrystallized with FGF2 (*19*) and with FGF2/FGFR1 (*23*) (see also refs *8* and *20*).

FGF2/p-PST·sU Interaction. Previous observations had shown that heparin protects FGF2 from proteolytic cleavage in a dose-dependent fashion and that the protective effect depends on the interaction of the glycosaminoglycan (GAG) with the growth factor and not with the proteolytic enzyme

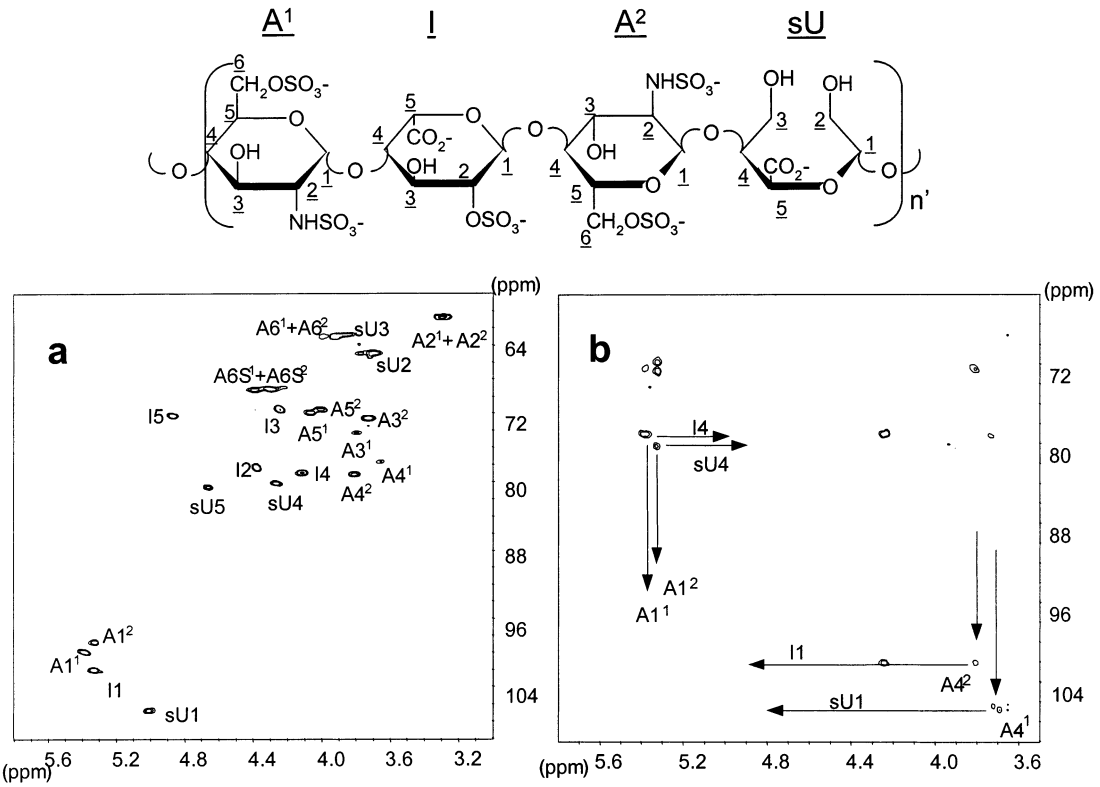

FIGURE 3: HSQC (a) and HMBC (b) spectra of **4** (p-PST·sU). Arrows indicate the proton-carbon interresidue connectivities of the tetrasaccharide repeating unit.

Table 2: Experimental Interproton NOE Values (%) for **1** and **4**

1		**4**	
$A^1$1−I4	2	$A^2$1−sU4	2
I1−$A^2$4	8	sU1−$A^1$4	8
I1−I5	0	sU^1−sU5	3

Table 3. ^{13}C Spin−Lattice Relaxation Times (T_2, ms) for **1** and **4**

	1	**4**
$A^1$1	51	118
$A^1$2	56	123
$A^1$3	61	119
$A^1$4	60	97
I1	57	100
I2	59	104
I3	58	124
I4	60	102
I5	35	86
sU1		127
sU4		116
sU5		97

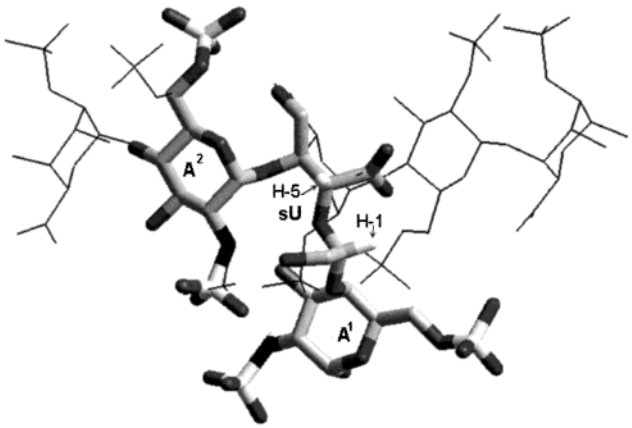

FIGURE 4: Molecular model of a trisaccharide segment of p-PST·sU (stick model) compared with unmodified heparin (thin line, ref *21*). For comparison purposes, the aminosugar residue A^2 is superimposed on the corresponding residue of heparin.

(*37*). On this basis, p-PST·sU was compared to unmodified heparin for the capacity to prevent FGF2 digestion by trypsin. As shown in Figure 5a, the two molecules exert a similar protective effect, with an ED_{50} equal to approximately 0.5 μg/mL. In agreement with its poor FGF2-binding capacity (*37*), *N*-acetyl heparin—taken as a negative control—was five times less effective.

In a second set of experiments, to evaluate further their ability to interact with FGF2, heparin, and p-PST·sU were assessed for the capacity to bind FGF2 and to prevent formation of the HSPG/FGF2/FGFR ternary complex (*48*). For this purpose, we utilized an experimental model in which disruption of the complex abolishes FGF2-mediated cell−cell attachment of HSPG-deficient CHO mutants transfected with FGFR1 (A745 CHO *flg*-1A cells) to wild-type CHO−K1 cells expressing HSPGs but not FGFR (*37*). In this model, a significant number of FGFR1-transfectants adhere to the HSPG-bearing monolayer in the presence of 30 ng/mL FGF2 (140 ± 20 cells/field) but not in the absence of the growth factor (20 ± 4 cells/field). Specificity of the cell−cell interaction was demonstrated by the inability of CHO mutants nontransfected with FGFR1 to adhere to the monolayer also in the presence of FGF2 (15 ± 3 cells/field). Again, both GAGs exerted a similar inhibitory activity on FGF2-mediated cell−cell adhesion whereas *N*-desulfated/*N*-acetylated heparin was ineffective (ID_{50} equal to 0.08 μg/mL, 0.05 μg/mL, and 50 μg/mL for unmodified heparin, p-PST-sU, and *N*-acetyl heparin, respectively) (Figure 5b).

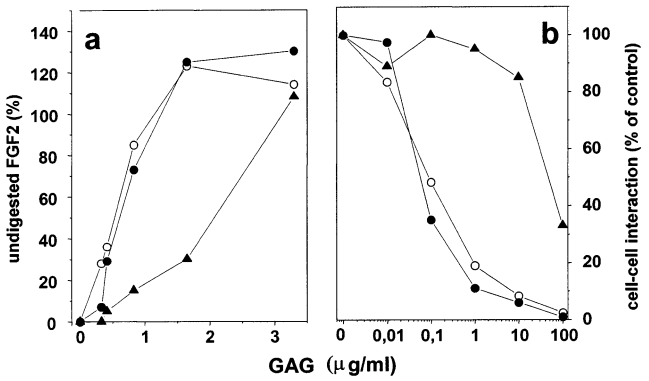

FIGURE 5: FGF2/p-PST·sU interaction. (a) Effect of p-PST·sU on FGF2 tryptic cleavage. FGF2 was incubated at 37 °C with trypsin in the presence of the GAG and its integrity was quantified by SDS−PAGE followed by computerized image analysis of the gel. (b) Effect of p-PST·sU on FGF2-mediated cell−cell adhesion. HSPG-deficient FGFR1 transfectants were added to wild-type CHO monolayers in the presence of FGF2 and the GAG and the bound cells were counted. GAGs: p-PST·sU (●), heparin (○), and *N*-acetyl heparin (▲).

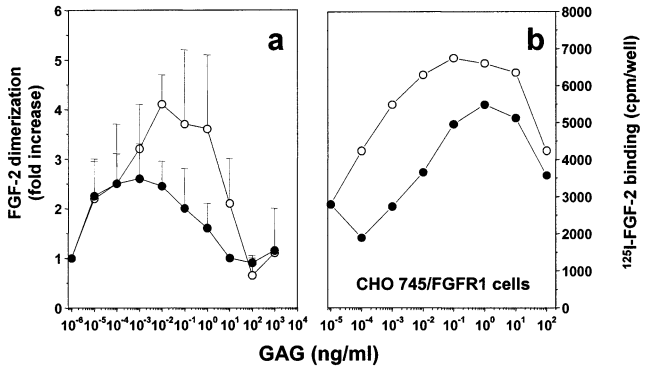

FIGURE 6: Effect of p-PST·sU on FGF2 oligomerization. (a) Chemically cross-linked FGF2 dimers were quantified after incubation of [^{125}I]FGF2 with the GAG. (b) Binding of [^{125}I]FGF2 to FGFR1, evaluated in A745 CHO flg-1A cells in the presence of the GAG. GAGs: p-PST·sU (●) or heparin (○). Each point is the mean of three determinations in duplicate.

Next, we compared the ability of the two GAGs to induce FGF2 oligomerization (*49*). As shown in Figure 6a, unmodified heparin stimulates the formation of the FGF2 dimer. The effect is dose-dependent and described by a bell-shaped curve. Indeed, heparin causes an increase in the amount of FGF2 dimer only at low doses, that is in the presence of a molar excess of FGF2 that favors the interaction of more than one molecule of FGF2 with a single GAG chain. No significant increase in the formation of FGF2 dimer is observed instead at a FGF2:heparin molar ratio equal or higher than 1:1, when only a single FGF2 molecule will interact with the GAG chain. As anticipated, the modifications of the structure of the heparin chain introduced in p-PST·sU caused a significant decrease ($p < 0.001$, paired two-population *t*-test) of the capacity of the GAG to induce FGF2 dimerization in the dose range between 0.001 and 1 ng/mL (Figure 6a). No induction of FGF2 dimerization was exerted by *N*-acetyl heparin (data not shown).

Previous observations had shown that heparin-induced oligomerization of FGF2 facilitate its interaction with FGFR and FGFR dimerization in cells lacking endogenous heparan sulfate (*50*). On this basis, we have compared p-PST·sU and unmodified heparin for the capacity to favor the interaction

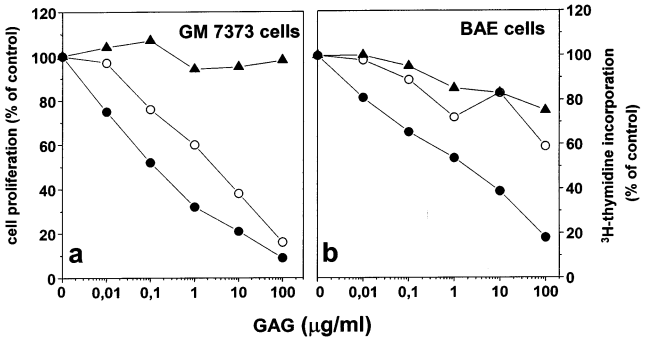

FIGURE 7: Effect of p-PST·sU on the mitogenic activity of FGF2 in cultured endothelial cells. (a) GM 7373 cells were incubated for 8 h with 10 ng/mL FGF2, added with the GAG for further 16 h and counted. (b) BAE cells were treated for 16 h with 30 ng/mL FGF2 in the presence of the GAG, and [^{3}H]thymidine incorporation was evaluated. Data are expressed as percentage of mitogenic activity exerted by FGF2 in the absence of any competitor. Each point is the mean of three to six determinations in duplicate. GAGs: p-PST·sU (●); heparin (○); *N*-acetyl heparin (▲).

of [^{125}I]FGF2 with FGFR1 in HSPG-deficient A745 CHO *flg*-1A transfectants. In agreement with its reduced capacity to facilitate FGF2 dimerization, p-PST·sU is approximately 100 times less potent than unmodified heparin in favoring the binding of [^{125}I]FGF2 to FGFR1 in A745 CHO flg-1A cells (Figure 6b).

Taken together, the above experiments indicate that p-PST·sU retains an FGF2-binding capacity similar to that exerted by unmodified heparin. As anticipated, however, p-PST·sU has lost, at least in part, the capacity to induce FGF2 oligomerization.

Effect of p-PST·sU on the Biological Activity Exerted by FGF2 on Endothelial Cells. To assess the effect of p-PST·sU on the biological activity exerted by FGF2 on endothelial cells in culture, fetal bovine aortic endothelial GM 7373 cells were incubated with FGF2 in the presence of increasing concentrations of unmodified heparin, *N*-acetyl heparin, or p-PST·sU and cell proliferation was evaluated 24 h thereafter. As shown in Figure 7a, p-PST·sU inhibits the mitogenic activity exerted by FGF2 with a potency significantly higher than the other GAGs under test (ID_{50} equal to 0.1 μg/mL, 2.0 μg/mL, and >100 μg/mL for p-PST·sU, unmodified heparin, and *N*-acetyl heparin, respectively). Also, p-PST·sU was a more potent inhibitor for FGF2-induced [^{3}H]-thymidine incorporation in BAE cells (ID_{50} equal to 1 μg/mL, 100 μg/mL, and >100 μg/mL for p-PST·sU, unmodified heparin, and *N*-acetyl heparin, respectively) (Figure 7b). Differences in HSPG composition of the cell surface may explain the different potency shown by each GAG in the two endothelial cell types.

These data prompted us to assess the capacity of p-PST·sU to exert an anti-angiogenic activity in vivo. The chick embryo chorioallantoic membrane (CAM) expresses FGF2 mRNA and protein (*51*, *52*) and endogenous FGF2 plays a limiting role in the development of the vascular system of this embryonic membrane (*51*). On this basis, the CAM represents an in vivo system suitable to assess the impact of putative anti-angiogenic FGF2 antagonists on blood vessel formation during development. As shown in Table 4, p-PST·sU exerts a significant inhibitory activity on blood vessel formation when applied at day 8 on the top of the CAM at

Table 4: Anti-Angiogenic Activity of Heparin Derivatives in the Chick Embryo CAM-Sponge Assay[a]

sample[b]	dose (μg/embryo)	angiogenesis inhibition (inhibited CAMs/total CAMs)
PBS		0/10
heparin	100	0/10
N-acetyl heparin	100	0/10
RO-heparin	100	3/10
p-PST·U	100	3/10
p-PST·sU	50	5/10
p-PST·sU	100	8/10

[a] Gelatin sponges containing the sample under test were applied on the CAM at day 8 of development. CAMs were scored macroscopically for inhibition of neovascularization at day 12 as described in Materials and Methods. [b] PBS, phosphate-buffered saline.

50 or 100 μg/embryo via a gelatin sponge implant (*43*). At day 12 of development this results in a 60% decrease in the average number of macroscopic blood vessels surrounding the implant (7 ± 2 vs 3 ± 1 total macroscopic blood vessels in control and p-PST·sU-treated sponges, respectively; $n = 10$). Histologic analysis of the CAMs followed by planimetric counting of microscopic blood vessels at the sponge-CAM boundary confirmed the inhibitory effect of p-PST·sU on angiogenesis (7 ± 3 vs 0 ± 0 microvessels per 0.125 mm^2 for control and p-PST·sU-treated CAMs, respectively, $n = 10$). Interestingly, p-PST·U (i.e., p-PST·sU before glycol-splitting) and a preparation of heparin that underwent partial glycol-splitting without previous partial 2-*O*-desulfation (RO−heparin), showed some antiangiogenic activity even though much lower than that exerted by the p-PST·sU derivative (Table 4). No macroscopic and microscopic inhibition of angiogenesis was observed in CAMs treated with unmodified or *N*-acetyl heparin (Table 4).

DISCUSSION

Biochemical studies with natural and synthetic glycosaminoglycan fragments have provided evidence that heparin and HS "activate" FGF2 by binding to the growth factor and by favoring oligomerization and formation of ternary complexes with its cellular receptors FGFRs (*2*). Oligosaccharides as small as tetrasaccharide are able to bind FGF2, provided they contain at least one $GlcNSO_3$ and one $IdoA2SO_3$ residue (*5*, *16*, *19*). However, only GAG chains longer than octadecasaccharide are able to activate FGFRs and to trigger mitogenic signals. Molecular modeling and X-ray diffraction studies have clearly shown that such a minimum size is required for building up assemblies of FGF and FGFR molecules (*8*, *20*). Indeed, in crystalline FGF2/FGFR1 assemblies the growth factor and its receptor generate a "basic canyon" which can ideally accommodate a relatively long heparin molecule in its extended helical conformation (*7*).

Although not all the sulfate groups of heparin/HS are essential for formation of 1:1 complexes with FGF2 (*13*−*15*), most of the complexes investigated thus far involve the trisulfated disaccharide sequences (TSD) constituted by alternating $IdoA2SO_3$ and $GlcNSO_36SO_3$ residues. These sequences, which are the chief product of biosynthesis of mammalian heparins and are much less represented in most HS species (*12*), are involved in binding of a large number of proteins (*10*, *20*, *53*). In pig mucosal heparins currently used in therapy, segments constituted by TSD sequences are on the average 8 disaccharide units long (*46*), i.e., long enough to bind to FGF2 and induce its dimerization and complexation with FGFRs. In the present work we showed that binding and induced activation of FGF2 can be modulated by generating sulfation gaps along the glycosaminoglycan chain, more specifically by removing sulfate groups from $IdoA2SO_3$ residues. We also showed that splitting the C(2)−C(3) bonds of the resulting nonsulfated IdoA residues together with those of preexisting nonsulfated uronic acids (GlcA and IdoA) generates flexible joints between the unmodified heparin sequences that confer FGF2 antagonist activity and anti-angiogenic capacity to the p-PST·sU heparin derivative. Relevant to this point is the observation that both partial 2-*O* desulfation and glycol-splitting are required for a potent anti-angiogenic activity of the heparin derivative. Indeed, RO-heparin (that underwent glycol-splitting in the absence of a partial 2-*O* desulfation) and the p-PST·U derivative (that underwent partial 2-*O* desulfation in the absence of glycol-splitting) exert only a very modest anti-angiogenic effect in the CAM assay when compared to p-PST·sU.

The role of local rigidity and flexibility along the heparin chains has been widely discussed in the context of the anticoagulant properties mediated by antithrombin III (AT) (*12*). The peculiar characteristics of IdoA residues to adopt more than one of two or three equienergetic conformations confer to IdoA-containing GAGs a "plasticity" that greatly enhances the binding ability of these polysaccharides (*12*, *53*). In fact, whereas FGF2 in its crystalline state with heparin tetra/hexasaccharides selects the chair $^1C_4$ conformation of an $IdoA2SO_3$ residue (*19*), heparin pentasaccharides select the skew-boat $^2S_0$ form of this residue in its complex with AT both in the crystalline state (*54*) and in solution. Glycol-splitting at the level of the preexisting nonsulfated uronic acid residues of heparin adds extra flexibility and conceivably additional protein-binding ability to the GAG chains, as deduced by enhanced lipoprotein-lipase (fat-clearing) and heparin cofactor II-mediated anticoagulant activities (*28*), and antiangiogenic activities (*56*) observed for periodate-oxidized/borohydride-reduced heparins (RO−heparins) as compared with unmodified heparins. It should be noted that periodate oxidation usually involves a dramatic drop of the AT-mediated anticoagulant activity of heparin, since it also involves splitting of the C(2)−C(3) bond of the essential GlcA residue of the pentasaccharide sequence constituting the active site for AT (*53*). As expected from both partial 2-*O*-desulfation and exhaustive glycol-splitting (the first modification impairing the HC2-mediated contribution, and the second one eliminating the AT-mediated contribution to the anticoagulant activity), the novel heparin derivative described in this paper has an anticoagulant activity even lower than reduced oxyheparin (RO−H, prevalently p-PST·U (data not shown).

Unfractionated, unmodified heparin modulates cell growth in general and angiogenesis in particular, sometimes with opposite effects depending on the cellular system and the type of assay (*57*). Since proliferation of endothelial cells is triggered by angiogenic signals, inhibition of growth of these cells is expected whenever FGF2 is not activated through oligomerization and formation of ternary complexes with FGFRs. However, the growth of endothelial cells is a

multifactorial event, and inhibition of FGFs (and/or their cellular receptors) does not always correspond to inhibition of cell growth. However, the effects of angiogenesis-inducing (or -inhibiting) factors can be different in different animal species (*58*). Whereas unmodified heparin inhibits growth of GM 7373 cells (Figure 6a), its effect on BAE cells is quite similar to the one of its *N*-acetylated derivative taken as negative control. In both cases p-PST·sU has a clear inhibiting effect, suggesting a prevailing mechanism of inhibition of FGF2.

The reported effects of unmodified heparin on angiogenesis and related events such as metastasis are paradoxical. On the basis of considerations that heparin sequences (or heparin fragments) smaller than octasaccharide are unable to generate FGF2-induced signaling, full-length heparin is expected to be pro-angiogenic. This is indeed the case in CAM models in the absence of angiostatic substances (*10*). In the presence of corticosteroids, heparin exerts a still unexplained antiangiogenic effect (*59*). In corticosteroid-free CAM models, heparin was reported to be either moderately antiangiogenic (*60*), inactive (*61*), or proangiogenic (*10*). Mechanisms other than direct inhibition of FGF2 may account for these apparent discrepancies. In fact, neovascularization usually involves also overexpression of the enzyme heparanase, which cleaves the HS chains of HSPG and releases FGF2 (and other growth factors) bound to these chains (*62*). Heparin and heparin-like substances are heparanase inhibitors. It is conceivable that the net effect on angiogenesis depends on the balance between inhibition of FGF2 release and direct inhibition of the released growth factor. In the present CAM model, whereas unmodified heparin did not affect angiogenesis, p-PST·sU exerted a marked antiangiogenic effect, a remarkable example of conversion of an angiogenesis activator to an inhibitor. The FGF2 antagonist and antiangiogenic activity of the novel heparin derivative sets the basis for the development of drug candidates in the therapy of angiogenesis-related diseases and solid tumors.

ACKNOWLEDGMENT

The authors thank Dr. Sara Guglieri for valuable assistance in molecular modeling and Prof. R. A. Lane for critical reading of the manuscript.

REFERENCES

1. Burgess, W. H., and Macaig, T. (1989) *Annu. Rev. Biochem. 58*, 576−606.
2. Ornitz, D. M. (2000) *Bioessays 22*, 108−112.
3. Bashkin, P. (1989) *Biochemistry 28*, 1737−1743.
4. Kato, M., Wang, H., Kainulainen, V., Fitzgerald, M. L., Ledbetter, S., Ornitz, D. M., and Bernfield, M. (1998) *Nat. Med. 4*, 691−697.
5. Moy, F. J., Safran, M., Seddon, A. P., Kitchen, D., Bölen, P., Aviezer, D., Yayon, A., and Powers, R. (1997) *Biochemistry 36*, 4782−4791.
6. Kwan, C.-P., Venkataraman, G., Shriver, Z., Raman, R., Liu, D., Qi, Y., Varticolavsaki, L., and Sasisekharan, R. (2000) *J. Biol. Chem. 276*, 23421−23429.
7. Plotnikov, A. N., Schlessinger, J., Hubbard, S. R., and Mohammadi, M. (1999) *Cell 98*, 641−650.
8. Pellegrini, M. (2001) *Curr. Opin. Struct. Biol. 11*, 629−634.
9. Lundin, L., Larsson, H., Kreuger, J., Kanda, S., Lindahl, U., Salmivirta, M., and Claesson-Welsh, L. (2000) *J. Biol. Chem. 275*, 24653−24660.
10. Ribatti, D., Gualandris, A., Bastki, M., Vacca, A., Roncali, L., and Presta, M. (1997) *J. Vasc. Res. 34*, 455−463.
11. Casu, B. (1985) *Adv. Carbohydr. Chem. Biochem. 43*, 51−132.
12. Casu, B., and Lindahl, U. (2001) *Adv. Carbohydr. Chem. Biochem. 57*, 159−208.
13. Maccarana, M., Casu, B., and Lindahl, U. (1993) *J. Biol. Chem. 268*, 23898−23905.
14. Turnbull, J. E., Fernig, D. G., Ke, Y., Wilkinson, M. C., and Gallagher, J. T. (1992) *J. Biol. Chem. 267*, 10337−10341.
15. Kreuger, J., Salmivirta, M., Sturiale, L., Giménez-Gallego, G. G., and Lindahl, U. (2001) *J. Biol. Chem. 276*, 30744−30752.
16. Ornitz, D. M., Herr, A. B., Nilsson, M., Westman, J., Svahn, C.-M., and Wachsman, G. (1995) *Science 268*, 432−436.
17. Kowenski, J., Duchaussoy, F., Bono, M., Herbert, J. M., Petitou, M., and Sinay, P. (1999) *Bioorg. Med. Chem. 7*, *8*, 1567−1580.
18. Waksman, G., and Herr, A. B. (1998) *Nat. Struct. Biol. 5*, 527−530.
19. Faham, S., Hileman, R. E., Fromm, J. R., Linhardt, R. J., and Rees, D. C. (1996) *Science 271*, 1116−1120.
20. Mulloy, B., and Linhardt, R. D. (2001) *Curr. Opin. Struct. Biol. 11*, 623−628.
21. Mulloy, B., Forster, M. J., Jones, C., and Davies, D. B. (1993) *Biochem. J. 293*, 849−858.
22. Venkataraman, G., Sasisekharan, V., Herr, A. B., Ornitz, D. M., Waksman, G., Cooney, C. L., Langer, L., and Sasisekharan, R. (1996) *Proc. Natl. Acad. Sci. U.S.A. 93*, 845−850.
23. Schlessinger, J., Plotnikov, A. N., Ibrahimi, O. A., Eliseenkova, A. V., Yeh, B. K., Yayon, A., Linhardt, R. J., and Mohammadi, M. (2000) *Mol. Cell 6*, 743−750.
24. Casu, B., Guerrini, M., Naggi, A., Torri, G., De-Ambrosi, L., Boveri, G., Gonella, S., Cedro, A., Ferro, L., Lanzarotti, E., Paternò, M., Attolini, M., and Valle, M. G. (1996) *Arzneim.-forsch. (Drug Res.) 46*, 472−477.
25. Harenberg, J., and De Vries, J. X. (1983) *J. Chromatogr. 261*, 287−292.
26. Cifonelli, J. (1966) *Carbohydr. Res. 2*, 150−156.
27. Isacchi, A., Statuto, M., Chiesa, L., Bergonzoni, L., Rusnati, M., Sarmientos, P., Ragnotti, G., and Presta, M. (1991) *Proc. Natl. Acad. Sci. U.S.A. 88*, 2628−2632.
28. Casu, B., Diamantini, G., Fedeli, G., Mantovani, M., Prino, G., Oreste, P., Pescador, R., Torri, G., and Zoppetti, G. (1985) *Arzneim.-forsch.* (*Drug Res.) 36*, 637−642.
29. Jaseja, M., Rej, R. N., Sauriol, F., and Perlin, A. S. (1989) *Can. J. Chem. 67*, 1449−1456.
30. Rej, R. N., and Perlin, A. S. (1990) *Carbohydr. Res. 200*, 437−447.
31. Piani, S., Casu, B., Marchi, E., Torri, G., Ungarelli, F., and Barbanti, M. (1993) *J. Carbohydr. Chem. 12*, 507−521.
32. Neville, G. A., Mori, F., Holme, K. R., and Perlin, A. S. (1989) *J. Pharm. Sci. 78*, 101−104.
33. Kay, L. E., Keifer, P., and Saaringen, T. (1992) *J. Am. Chem. Soc. 114*, 10663−10665.
34. Summers, M. F., Marzilli, L. G., and Bax, A. (1986) *J. Am. Chem. Soc. 108*, 4285−4294.
35. Kay, L. E., Nicholson, L. K., Delaglio, F., Bax, A., and Torchia, D. A. (1992) *J. Magn. Res. 97*, 359−375.
36. McDonalds, D. Q., and Still, W. C. (1992) *Tetrahedron Lett. 33*, 7743−7759.
37. Coltrini, D., Rusnati, M., Zoppetti, G., Oreste, P., Isacchi, A., Caccia, P., Bergonzoni, L., and Presta, M. (1993) *Eur. J. Biochem. 214*, 51−58.
38. Grinspan, J. B., Stephen, N. M., and Levine, E. M. (1983) *J. Cell. Physiol. 114*, 328−338.
39. Liekens, S., Leali, D., Neyts, J., Esnouf, R., Rusnati, M., Dell'Era, P., Maudgal, P. C., De Clercq, E., and Presta, M. (1999) *Mol. Pharmacol. 56*, 204−213.
40. Esko, J. D. (1991) *Curr. Opin. Cell. Biol. 3*, 805−816.
41. Moscatelli, D. (1992) *J. Biol. Chem. 267*, 25803−25809.
42. Rusnati, M., Urbinati, C., and Presta, M. (1997) *J. Cell. Physiol. 154*, 152−161.
43. Ribatti, D., Gualandris, A., Bastaki, M., Vacca, A., Roncali, L., and Presta, M. (1997) *Dev. Biol. 170*, 39−49.
44. Brooks, P. C., Clark, R. A. F., and Cheresh, D. A. (1994) *Science 264*, 569−571.
45. Faham, S., Linhardt, R. J., and Rees, D. C. (1998) *Curr. Opin. Struct. Biol. 8*, 578−586.
46. Fransson, L.-Å., Malmström, A., and Sjöberg, R. G. (1980) *Carbohydr. Res. 80*, 131−145.

47. Mascellani, G., Liverani, L., Bianchini, P., Parma, B., Torri, G., Bisio, A., Guerrini, M., and Casu, B. (1993) *Biochem. J.*, 639−648.
48. Richard, C., Liuzzo, J. P., and Moscatelli, D. (1995) *J. Biol. Chem. 270*, 24188−24196.
49. Ornitz, D. M., Yayon, A., Flanagan, J. G., Svahn, C. M., Levi, E., and Leder, P. (1992) *Mol. Cell. Biol. 12*, 240−247.
50. Spivak-Krolzman, T., Lemmon, M. A., Dikic, I., Ladbury, J. E., Pinchasi, D., Huang, J., Jaye, M., Crumley, G., Schlessinger, J., and Lax, I. (1994) *Cell 79*, 1015−1024.
51. Ribatti, D., Gualandris, A., Bastaki, M., Vacca, A., Roncali, L., and Presta, M. (1997) *J. Vasc. Res. 34*, 445−463.
52. Ribatti, D., Bertossi, M., Nico, B., Vacca, A., Ria, R., Riva, A., Roncali, L., and Presta, M. (1998) *J. Submicrosc. Cytol. Pathol. 30*, 127−136.
53. Conrad, E. (1998) *Heparin binding proteins*, Academic Press, San Diego.
54. Jin, L., Abrahams, J.-P, Petitou, M., Pike, R. N., and Carrell, R. W. (1997) *Proc. Natl. Acad. Sci. U.S.A.*, 4683−4688.
55. Hricovini, M., Guerrini, M., Bisio, A., Torri, G., Petitou, M., and Casu, B. (2001) *Biochem. J. 359*, 265−272.
56. Lapierre, F., Holme, K., Lam, L., Tressler, L. J., Storm, N., Wee, J., Stack, R. J., Castellot, J., and Tyrrell, D. J. (1996) *Glycobiology 6*, 355−366.
57. Folkman, J., and Ingber, D. E. (1987) in *Heparin* (Lane D. A., and Lindhal, U., Eds.) pp 317−333, Edward Arnold, London.
58. Griffioen, A. W., and Molema, G. (2000) *Pharmacol. Rev. 52*, 237−268.
59. Folkman, J., Langer, L., Linhardt, R. J., Haudenschield, C., and Taylor, S. (1983) *Science 221*, 719−725.
60. Jakobson, Å. M., and Hahnenberg, R. (1991) *Pharmacol. Toxicol. 64*, 122−126.
61. Taylor, S., and Folkman, J. (1982) *Nature 297*, 307−312.
62. Elkin, M., Ilan, N., Ishai-Michaeli, R., Friedman, Y., Papo, O., Pecker, I., and Vlodavsky, I. (2001) *FASEB J. 15*, 1661−1663.
63. Ishai-Michaeli, R. T., Svahn, C. M., Weber, M., Chajek-Shaul, T., Korner, G., Ekre, H.-P., and Vlodavsky, I. (1992) *Biochemistry 31*, 2080−2088.

BI020118N